Anatomy of a Gel. Amino Acid Derivatives That Rigidify Water at Submillimolar Concentrations

Fredric M. Menger* and Kevin L. Caran

Contribution from the Department of Chemistry, Emory University, 1515 Pierce Drive, Atlanta, Georgia 30322

Received May 15, 2000. Revised Manuscript Received September 20, 2000

Abstract: On the basis of suggestive X-ray data, 14 aroyl L-cystine derivatives were designed, synthesized, and examined for their ability to gelate water. Several members of this amino acid family are remarkably effective aqueous gelators (the best being one that can rigidify aqueous solutions at 0.25 mM, ca. 0.01%, in less than 30 s!). A few of the analogues separate from water as crystals, indicating a close relationship between gelation and crystallization. All effective gelators self-assemble into fibrous structures that entrain the solvent in the capillary spaces among them. Hydrogen-bonding sites on the compounds that might stabilize the fibers were identified from specific substitutions that replace a hydrogen donor with a methyl group, enhance the hydrogen-accepting ability of a carbonyl oxygen, or promote the hydrogen-donating ability of an amide proton. The structural variations were characterized via minimal gelation concentrations and times, X-ray crystallography, light and electron microscopy, rheology, and calorimetry. The multiple techniques, applied to the diverse compounds, allowed an extensive search into the basis of gelation. It was learned, for example, that the compound with the lowest minimum gelator concentration and time also has one of the weakest gels (i.e., it has a low elastic modulus). This is attributed to kinetic effects that perturb the length of the fibers. It was also argued that π/π stacking, the carboxyl carbonyl (but not the carboxyl proton), and solubility factors all contribute to the stability of a fiber. Polymorphism also plays a role. Rheological studies at different temperatures show that certain gels are stable to a 1-Hz, 3-Pa oscillating shear stress at temperatures as high as 90 °C. Other gels have a "catastrophic" break at lower temperatures. Calorimetric data indicate a smooth transition from gel to sol as the temperature is increased. These and other issues are discussed in this "anatomy" of a gel.

Introduction

Any child who has eaten a gelatin desert, or experienced "sheer-thinning" by squirting it through his teeth, is familiar with the gel state. Actually, gels are found not only in food but throughout Nature. Protoplasm, for example, is a gel. How strange it is that, despite gels being so commonplace, hard data on their molecular structure is in limited supply. There are several reasons for this: Gelators of water are usually large molecules (i.e., proteins and polymers) whose complicated intermolecular associations are difficult to define. Moreover, the interactions are generally not static but can change (often irreversibly) with time, heat, or stress. And, of course, gels do not lend themselves to atomic resolution X-ray analysis, the main source of our most precise structural information.

We have learned how to prepare clear gels in less than 30 s via extremely dilute (0.25 mM!) aqueous solutions of amino acid derivatives. The story of how we came to design such simple gelators is the subject of the present paper. Although we do not know the structure of our gels with X-ray-like detail, we now have a basic understanding of how the compounds rigidify water. But before beginning the story (which will take us into the realm of microscopy and rheology), let us first give a succinct overview of gel chemistry.

A wide variety of nonpolymeric compounds have been encountered that create colloidal gels in organic media.[1−4] The great majority have been discovered by chance and include diverse structural types such as long-chain *n*-alkanes,[5] steroid/aromatic conjugates,[6−9] carbohydrate derivatives,[10−13] dendrimers,[14] and two-component systems.[15−17] Nonpolymeric compounds capable of gelating water include arborols[18,19] and amphiphiles;[20−22] they are less common because 55 M water competes for hydrogen-bonding sites, a major associative element. One particularly interesting gelator, a diammonium gemini surfactant,[23] is able to form gels in both water and

(1) For a recent review of low-molecular-mass organic gelators, see: Terech, P.; Weiss, R. G. *Chem. Rev.* **1997**, *97*, 3133.
(2) Bhattacharya, S.; Acharya, S. N. G. *Chem. Mater.* **1999**, *11*, 3121.
(3) Aoki, M.; Nakashima, K.; Kawabata, H.; Tsutsui, S.; Shinkai, S. *J. Chem. Soc., Perkin Trans. 2* **1993**, *3*, 347.
(4) Terech, P.; Ostuni, E.; Weiss, R. G. *J. Phys. Chem.* **1996**, *100*, 3759.
(5) Abdallah, D. J.; Weiss, R. G. *Langmuir* **2000**, *16*, 352.
(6) Geiger, C.; Stanescu, M.; Chen, L.; Whitten, D. G. *Langmuir* **1999**, *15*, 2241.
(7) Terech, P.; Ostuni, E.; Weiss, R. G. *J. Phys. Chem.* **1996**, *100*, 3759.
(8) Lin, Y.-c.; Kachar, B.; Weiss, R. G. *J. Am. Chem. Soc.* **1989**, *111*, 5542.
(9) Lin, Y.-c.; Weiss, R. G. *Macromolecules* **1987**, *20*, 414.
(10) Watase, M.; Nakatani, Y.; Itagaki, H. *J. Phys. Chem. B* **1999**, *103*, 2366.
(11) Hafkamp, R. J. H.; Feiters, M. C.; Nolte, R. J. M. *J. Org. Chem.* **1999**, *64*, 412.
(12) Amanokura, N.; Yoza, K.; Shinmori, H.; Shinkai, S.; Reinhoudt, D. N. *J. Chem. Soc., Perkin Trans. 2* **1998**, 2585.
(13) Yamasaki, S.; Ohashi, Y.; Tsutsumi, H.; Tsujii, K. *Bull. Chem. Soc. Jpn.* **1995**, *68*, 146.
(14) Jang, W.-D.; Jiang, D.-L.; Aida, T. *J. Am. Chem. Soc.* **2000**, *122*, 3232.
(15) Inoue, K.; Ono, Y.; Kanekiyo, Y.; Ishi-I. T.; Yoshihara, K.; Shinkai, S. *J. Org. Chem.* **1999**, *64*, 2933.
(16) Maitra, U.; Kumar, P. V.; Chandra, N.; D'Souza, L. J.; Prasanna, M. D.; Raju, A. R. *Chem. Commun.* **1999**, 595.
(17) Hanabusa, K.; Miki, T.; Taguchi, Y.; Koyama, T.; Shirai, H. *J. Chem. Soc., Chem. Commun.* **1993**, 1382.

10.1021/ja0016811 CCC: $19.00
Published on Web 11/10/2000

organic solvents.[24] All of these systems can be considered "physical gels" in that noncovalent intermolecular associations are responsible for gelation.[25]

Gels are semirigid colloidal systems rich in liquid. Most gels consist of long fibers that have been self-assembled as a result of the usual array of supramolecular forces (hydrogen-bonding, aromatic stacking, electrostatics, etc.). Noncovalent cross-links among the fibers and/or mechanical entanglements create a three-dimensional network. Solvent is entrapped within the interstices, thereby imparting rigidity to the system. Other gel morphologies, such as densely packed vesicles,[26−28] have also been identified.

Two not entirely distinct theories have been advanced to explain the mechanism of the sol-to-gel transition that occurs, for example, upon cooling a hot gelator solution. The first, championed by Bradford in the 1920s,[29] maintains that gelation is a type of incomplete crystallization (the gel consisting of microcrystalline forms surrounded by solvent). Alternatively, a gel may be formed by noncrystalline aggregates which, as mentioned, entrain the dispersing medium in the capillary spaces between them.

The thermal stability of a gel may be probed by observing spectroscopic features (NMR,[3,12,16] UV,[16,20] CD,[8,9,12] fluorescence[8,9]), thermal properties (DSC[3,5,10,11]), and physical state[3,5,11,30] over a range of temperatures. Gel-to-sol transition temperatures (T_{GS}) and the (not necessarily identical) sol-to-gel transition temperatures (T_{SG}) are obtained by these means. A gel's macroscopic physical characteristics are quantified rheologically from a sample's response to an oscillating stress.[1,21,26−28,31−33]

It is now possible to return to our amino acid-based gelators that rigidify water at remarkably low concentrations. The story begins in 1921, when Gortner and Hoffman discovered that dibenzoyl-L-cystine (**1**) forms a strong aqueous gel.[34,35] It was an amazing discovery. Only 0.2% **1**, corresponding to approximately 12 000 waters/gelator molecule, suffices to create a hydrogel.

Typically, the gels are prepared by dissolving **1** in 5 mL of hot ethanol and then diluting to 100 mL with water. Gortner−Hoffman gels remained unexplored by modern instrumentation until, in 1978, we applied ^{13}C NMR to the system.[36] It was demonstrated from spin−lattice relaxation times (T_1) and from line widths that highly concentrated (0.3−0.6 M) gelated **1** exists as two distinct molecular types: (a) a species that possesses T_1 values and line widths expected for a monomer and (b) an aggregated species whose ^{13}C resonances are broadened to the point of unobservability by dipolar interactions at these relatively high gelator concentrations. The results are best interpreted in terms of soluble monomer, entrapped within a microcrystalline network, that neither exchanges with the network (on the NMR time scale) nor experiences difficulty moving about the small aqueous domains.

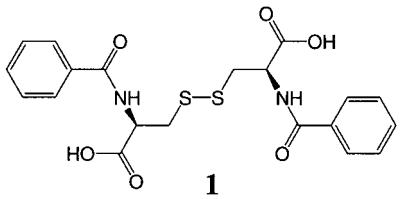

1

Seventeen years went by, and then, in the course of synthesizing various aroyl-L-cystines, crystals of X-ray quality were obtained from di(*p*-toluoyl)-L-cystine.[37] We asked of our crystals (as did others[38]) the perennial question of whether solid-state properties actually reflect solution properties. We were inclined to answer affirmatively because, for one thing, the crystal showed a "fibrous" molecular orientation. But there was another reason for taking the X-ray structure seriously. By applying Occam's razor and assuming a relationship between crystal and gel, we could examine the intermolecular forces within the crystal and, thereby, design an even better gel by enhancing those forces. If, on the other hand, we had assumed that the crystal structure was irrelevant to the gel, then the future experimental course of action would have been less motivated. In any event, the strategy succeeded. Without reproducing the original X-ray picture, let us summarize the thought sequence, derived therefrom, that led us to the design and synthesis of our powerful new gelators.

The X-ray picture showed a linear stacking of the di(*p*-toluoyl)-L-cystine molecules in which each unit is connected to the one above and below it by two hydrogen bonds each.[39] As can be seen in the structure below, amide-NH's serve as the hydrogen-bond donors, whereas carboxyl carbonyls serve as the hydrogen-bond acceptor. Since the aromatic rings in the "fibrous" array are situated one above another, π/π stacking might further contribute to the fiber's stability. In any event, it was apparent that if a similar packing existed in the gel, then a stronger gel could be produced by accentuating the hydrogen-bonding acceptor capabilities of the carbonyl. This could be readily accomplished by converting the α-carboxyl into a primary α-carboxamide. Similarly, the amide-NH would become a better hydrogen-bonding donor via the presence of electron-withdrawing groups on the aromatic ring.

(18) Newcome, G. R.; Baker, G. R.; Arai, S.; Saunders, M. J.; Russo, P. S.; Theriot, K. J.; Moorefield, C. N.; Rogers, L. E.; Miller, J. E.; Lieux, T. R.; Murray, M. E.; Phillips, B.; Pascal, L. *J. Am. Chem. Soc.* **1990**, *112*, 8458.

(19) Newcome, G. R.; Baker, G. R.; Saunders, M. J.; Russo, P. S.; Gupta, V. K.; Yao, Z.-q.; Miller, J. E.; Bouillion, K. *J. Chem. Soc., Chem. Commun.* **1986**, 752.

(20) Kimura, T.; Shinkai, S. *Chem. Lett.* **1998**, 1035.

(21) Clausen, T. M.; Vinson, P. K.; Minter, J. R.; Davis, H. T.; Talmon, Y.; Miller, W. G. *J. Phys. Chem.* **1992**, *96*, 474.

(22) Furhop, J.-H.; Schnieder, P.; Rosenberg, J.; Boekema, E. *J. Am. Chem. Soc.* **1987**, *109*, 3387.

(23) For gemini surfactants, see: Menger, F. M.; Littau, C. *J. Am. Chem. Soc.* **1991**, *113*, 1451. Menger, F. M. Keiper, J. S. *Angew. Chem., Int. Ed.* **2000**, in press.

(24) Oda, R.; Huc, I.; Candau, S. J. *Angew. Chem., Int. Ed.* **1998**, *37*, 2689.

(25) A *chemical gel*, on the other hand, is defined as one in which the gelator aggregates are held together by covalent cross-links, trapping the liquid phase within a non-thermoreversible three-dimensional polymeric structure.

(26) Gradzielski, M.; Bergmeier, M.; Muller, M.; Hoffman, H. *J. Phys. Chem. B* **1997**, *101*, 1719.

(27) Hoffman, H.; Thunig, C.; Schmiedel, P.; Munkert, U. *Faraday Discuss.* **1995**, *101*, 319.

(28) Hoffman, H.; Thunig, C.; Schmiedel, P.; Munkert, U. *Langmuir* **1994**, *10*, 3972.

(29) Bradford, S. C. *Biochem. J.* **1921**, *15*, 553.

(30) Tan, H.-M.; Moet, A.; Hiltner, A.; Baer, E. *Macromolecules* **1983**, *16*, 28−34.

(31) Ikeda, S.; Foegeding, E. A.; Hagiwara, T. *Langmuir* **1999**, *15*, 8584.

(32) Aggeli, A.; Bell, M.; Boden, N.; Keen, J. N.; Knowles, P. F.; McLeish, T. C. B.; Pitkeathly, M.; Radford, S. E. *Nature* **1997**, *386*, 259.

(33) Aggeli, A.; Bell, M.; Boden, N.; Keen, J. N.; McLeish, T. C. B.; Nyrkova, I.; Radford, S. E.; Semenov, A. *J. Mater. Chem.* **1997**, *7*, 1135.

(34) Gortner, R. A.; Hoffman, W. F. *J. Am. Chem. Soc.* **1921**, *43*, 2199. The gelation of dibenzoyl-L-cystine had been noted earlier [Brezinger, *Z. Phisiol. Chem.* **1892**, *16*, 537], but Gortner and Hoffman, who reported observing this gel before consulting this earlier work, were the first to study its properties.

(35) Wolfe, C. G. L.; Rideal, E. K. *Biochem. J.* **1922**, *16*, 548.

(36) Menger, F. M.; Venkatasubban, K. S. *J. Org. Chem.* **1978**, *43*, 3143.

(37) Menger, F. M.; Yamasaki, Y.; Catlin, K. K.; Nishimi, T. *Angew. Chem., Int. Ed. Engl.* **1995**, *34*, 585.

(38) Ostuni, E.; Kamaras, P.; Weiss, R. G. *Angew. Chem., Int. Ed. Engl.* **1996**, *35*, 1324.

(39) **2** was recrystallized from methanol/ethyl acetate, see ref 37.

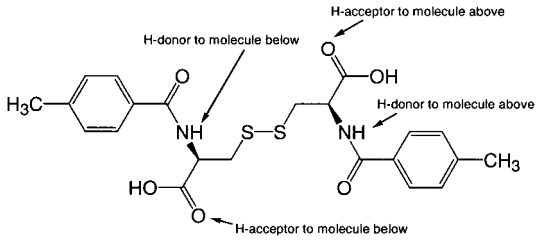

The consequences of these modifications, plus those of several other modifications, is the focus of the ensuing discussion. Table 1 lists our 14 L-cystine derivatives, and Scheme 1 summarizes their synthesis. Although all of these compounds are aromatic derivatives, we have also examined the diacetyl derivative (which fails to form a gel) and the dioctanoyl derivative (which does gelate).[40]

Results and Discussion

Synthesis of the Gelators. Access to our colloidal systems was obviously made possible through the intervention of synthetic organic chemistry. We are indebted to the discipline because only with the aid of organic synthesis can key relationships between colloidal activity and molecular structure ever be established.

Preparation of L-cystine derivatives **1**,[41] **2**,[37] and **3** (Table 1, Scheme 1) was accomplished by acylation under Schotten−Bauman conditions. Primary amide derivatives **4**−**10** were obtained in two steps. L-Cystine dimethyl ester dihydrochloride was first reacted with liquid ammonia, yielding intermediate **15** after acidification.[42] This was followed by acylation of the primary amide with an appropriate acyl chloride using the Schotten−Bauman reaction with sodium acetate as the base for **4** and **5**, or with triethylamine in chloroform/DMSO for **6**−**10**. Secondary amide **11** was prepared in a manner analogous to **5** except that methylamine was substituted for ammonia in the first step. Despite several attempts, extending the method to make the tertiary amide with dimethylamine was unsuccessful. Thus, dimethylamide **12** was synthesized in four steps from commercial bis(benzyloxycarbonyl)-L-cystine: The diacyl chloride[43] was prepared with PCl_5 in ether at 0 °C; the solution was subsequently condensed with dimethylamine in ether at −78 °C. Deprotection of the resulting dimethylamide **17** with HBr in acetic acid afforded diamine salt **18**, which in turn was benzoylated to **12**. L-Cystine derivative **13** (the only member of Table 1 with a tertiary α-amido group) was obtained by the reduction of *R*-(−)-thiazolidine-4-carboxylic acid with sodium/liquid ammonia followed first by air oxidation to the disulfide (**19**)[44] using catalytic iron(II) sulfate and then by Schotten−Bauman benzoylation.[45] Derivative **14**, the only ester in the group, was made by benzoylation of L-cystine dimethyl ester dihydrochloride.

Except for derivatives **4** (from which X-ray-quality crystals were obtained after chromatography on a silica column with ether as the eluant) and **12** (which was recrystallized from MeOH/H_2O), the compounds in Table 1 were purified by trituration in hot methanol, water, or ether. The identity and purity of all final products were verified by elemental analysis, MS, ^1H and ^{13}C NMR after the solids were dried in a vacuum oven over P_2O_5. Full details are given in the Experimental Section.

Table 1. Derivatives of L-Cystine

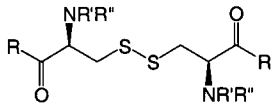

	R	R′	R″
1	OH	H	benzoyl
2	OH	H	*p*-toluoyl
3	OH	H	*p*-nitrobenzoyl
4	NH_2	H	*p*-nitrobenzoyl
5	NH_2	H	benzoyl
6	NH_2	H	*p*-toluoyl
7	NH_2	H	*p*-anisoyl
8	NH_2	H	3,5-dimethoxybenzoyl
9	NH_2	H	3,5-dinitrobenzoyl
10	NH_2	H	2-naphthoyl
11	$NHCH_3$	H	benzoyl
12	$N(CH_3)_2$	H	benzoyl
13	OH	CH_3	benzoyl
14	OCH_3	H	benzoyl

General Characteristics. Since the compounds in Table 1 are water-insoluble, a water-miscible cosolvent was required to prepare the aqueous gels. Ethanol could not be used as a cosolvent (as it had been in the past with carboxylic acids) because the corresponding amides in Table 1 do not dissolve, even in hot ethanol. All the L-cystine derivatives are, however, soluble in DMSO, which was therefore used throughout our study as a cosolvent and as a dispersant that allows the gelator molecules to spread throughout the water prior to fiber formation. As will be seen, various concentrations of DMSO (5−25% v/v) were examined in order to assess the effect of cosolvent upon gelation. Typically, the compounds in Table 1 were dissolved in warm DMSO, hot water was added, and cooling was allowed to take place from about 90 °C to room temperature. It may be no accident that this gelation procedure resembles a crystallization protocol. Cooling lowers the solubility and promotes self-assembly into a sparingly soluble network in the gel case and into an insoluble ordered array in the case of a crystal.

A general scanning of our 14 potential gelators was carried out prior to our performing more quantitative measurements. It should be stated at the outset that having 14 compounds on hand gave us great versatility with regard to understanding the effects of structure upon gelation. Unfortunately, it also gives the reader a collection of organic structures which, obviously, cannot be kept continuously in mind. Thus, the reader will be forced to refer frequently to Table 1 as we mention one particular gelator or the other. In any event, Table 2 gives the gross appearance of the gels made in 95% H_2O/5% DMSO. The "properties" column classifies the gels into such categories as G (stable to inversion of the container) and J (a jelly unstable to inversion). The "concentration" column gives the approximate minimum gelator concentration necessary for gelation. As can be seen, gelator **10** (the naphthoyl amide) gelates at only 0.25 mM. We know of no other low-molecular-weight gelator that competes with this number. In the "appearance" column, we reveal whether a gel is clear, translucent, or opaque at the minimum gel concentration. Finally, the "gel time" column lists the approximate time required for the minimum gelator concentration to gelate after mixing of the components at about 90 °C. Gelator **10** rigidifies water in less than 30 s, while most of

(40) McSorley, K. S. Master's Thesis, Emory University, Atlanta, GA, 1991.
(41) Martin, T. A. *J. Med. Chem.* **1969**, *12*, 950.
(42) Martin, T. A.; Causey, D. H.; Sheffner, A. L.; Wheeler, A. G.; Corrigan, J. R. *J. Med. Chem.* **1967**, *10*, 1172.
(43) Gustus, E. L. *J. Org. Chem.* **1967**, *32*, 3425.
(44) Keller-Schierlein, W.; Mihailovie, M. Lj.; Prelog, V. *Helv. Chim. Acta* **1959**, *26*, 305.
(45) Bloch, K.; Clarke, H. T. *J. Biol. Chem.* **1938**, *125*, 275.

Scheme 1. Synthesis of l-Cystine Derivatives

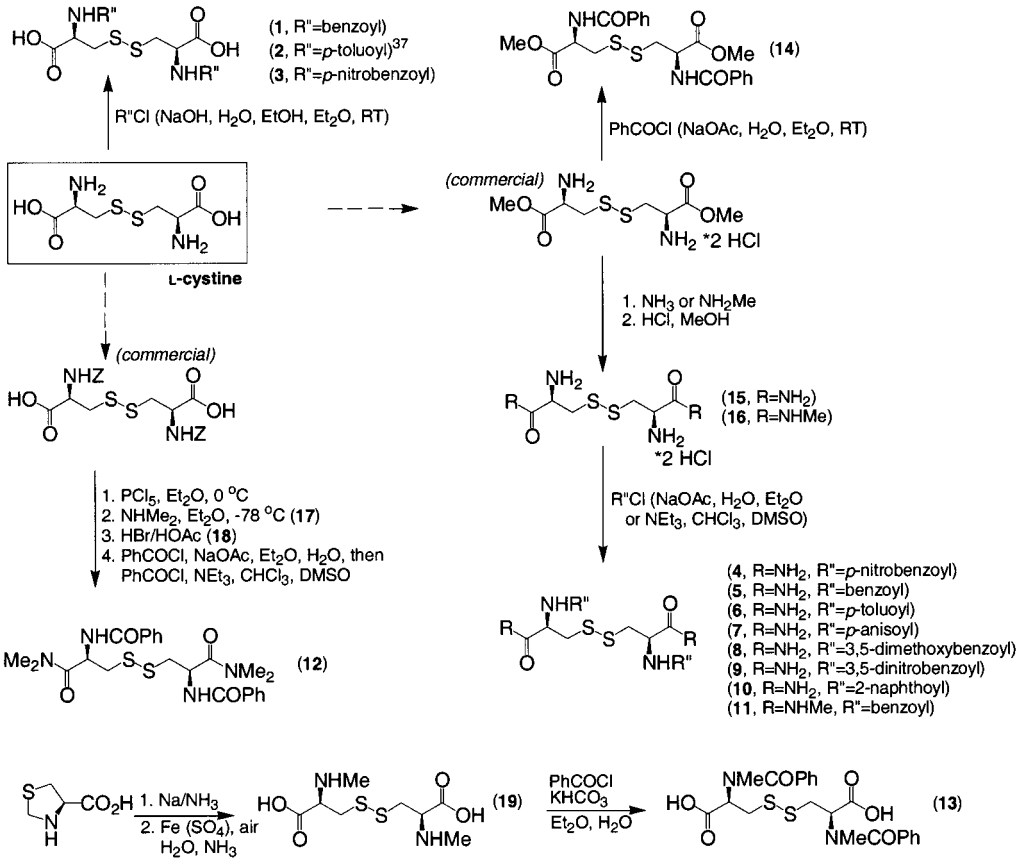

Table 2. Behavior of L-Cystine Derivatives in Water/DMSO[a]

compd	properties[b]	concn (mM)[c]	appearance[d]	gel time
1	G	3.0	C	2−3 h
2[f]	R			
3	R			
4	G,J[g]	2.0	T	5−10 min
5	G	0.5	C	3−5 min
6	G	0.5	C	1−2 min
7	G	2.0	O	5−10 min
8	P[h]			
9	J			
10[i]	G	0.25	C	<30 s
11	G	2.0	T	20−30 min
12	R			
13	P			
14	G	2.0	O	3−5 min

[a] The gelation was tested in 95% H_2O/5% DMSO unless otherwise noted. [b] G: forms a gel which is stable to inversion. J: forms a gel-like solid ("jelly") which is unstable to inversion. P: precipitates. R: recrystallizes. [c] Minimum concentration required for gelation. [d] Appearance of gel at minimum gel concentration. C: clear; little or no appearance of a solid phase. T: translucent; some small crystallites or slightly opaque regions. O: opaque. [e] Approximate time required for gelation at minimum concentration after mixing components at ~90 °C (allowing them to cool to room temperature in air). [f] From ref 37. [g] Compound **4** displayed inconsistent behavior. [h] Precipitated as fibrous balls (see text). [i] 25% DMSO was required to prepare gels from **10** (see text).

the other amides do so in minutes. Increasing the gelator concentration can substantially reduce these gelation times even further.

Figure 1 offers a visual respite from the tabular information in Table 2. Three gels of **5** (0.5, 1.0, and 3.0 mM in 90% H_2O/10% DMSO) are all seen to be stable to inversion. The gel becomes opaque only at the highest concentration.

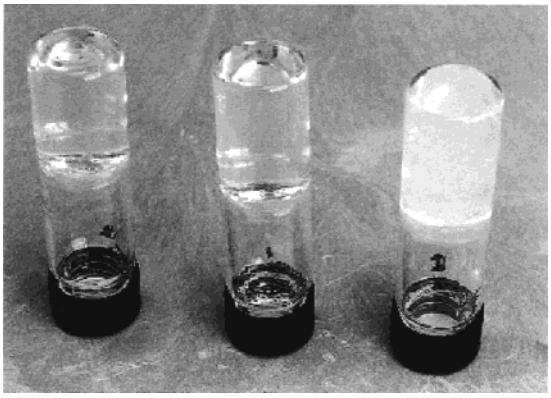

Figure 1. Three gels composed of **5** (0.5, 1.0, and 3.0 mM, left to right) which are stable when inverted as shown (90/10 DMSO/water). Note the increased opacity of the 3.0 mM gel.

Returning now to Table 2, we summarize below the structure/activity relationships derived therefrom. For ease of discussion, the terms "acid" or "amide" will be used according to the derivitization state of the L-cystine α-carboxyls (R in Table 1). All our compounds of course possess, additionally, two aromatic amides (R″ in Table 1).

(a) Since ester **14** can form gels, the carboxyl proton in the parent compound **1** is not an essential intermolecular hydrogen-bonding site within the gel network.

(b) All other successful gelators (**4**−**7**, **10**, and **11**) are amides of the carboxyl group (R = amino in Table 1). They gelate at lower concentrations (0.25−2.0 mM) and at faster times (from <30 s to ~30 min) than the parent carboxylic acid **1**. Since an amide carbonyl is a stronger hydrogen-bonding carbonyl than a carboxyl carbonyl, we surmise (as discussed in the Introduction) that the carbonyl oxygen serves as a key hydrogen-bonding

unit in the self-assembly of the gelating fibers. One must also recognize that the amides tend to be less water-soluble than the parent acid. This will promote both the rate and extent of gelation among the amides.

(c) Comparison of **5**, **11**, and **12** shows that having two methyls (but not one) on the α-carboxamide group nitrogen destroys gelation. Unless an α-carboxamide proton is necessary for hydrogen-bonding (and there is no independent evidence for this), the two methyl groups may simply be exerting a deleterious steric effect.

(d) Compound **10**, with primary amides and with naphthoyls on the α-amino group, is the best gelator in the series. In fact, **10** gelates so rapidly (even before all the hot water could be added) that it was necessary to prepare the gel in 25% rather than 5% DMSO (the only gelator so handled in Table 2). Even with this modification, **10** forms a clear gel in a matter of seconds. One is tempted to conclude that π/π stacking of the large naphthalene groups stabilizes the gel fibers. Low water solubility of **10** no doubt also plays a role.

(e) Placing methyl or nitro groups on **1**'s aromatic rings converts **1** from a gelator into crystal-forming compounds **2** and **3**. Even a seemingly innocuous *p*-methyl group is seen to affect the gel/crystal relationship. The nondependence of the gel/crystal relationship on the electron-withdrawing ability of the aromatic substituent, and thus the NH hydrogen-bonding acidity, demonstrates the complexity of factors dictating crystallinity.

(f) In contrast to the acids, altering the aromatic rings of amide **5** did not necessarily destroy their gelating ability. Substituents on the aroyl groups of the primary amides (i.e., *p*-NO_2 in **4**; *p*-CH_3 in **6**; *p*-OCH_3 in **7**; 3,5-di-OCH_3 in **8**; and 3,5-di-NO_2 in **9**) show no obvious trend compared to that of unsubstituted **5**. Thus, as seen in Table 2, neither the highly electron-rich **8** nor the electron-poor **9** is a good gelator (forming a precipitate and a fluid "jelly", respectively). This was surprising since we had expected from our X-ray data (see Introduction) that the aroyl amide NH protons were engaged in hydrogen-bonding and that, therefore, the nitro groups should be gel-strengthening. However, it must be borne in mind that there is a delicate balance between gelation and crystallization in accord with Bradford's "incomplete crystallization" theory. Apparently, a relatively minor structural change can tip the balance in an unpredictable manner.

To summarize: Gelation is undoubtedly the product of intermolecular forces, particularly hydrogen-bonding. Since it is known from previous work that replacing −S−S− with $-CH_2CH_2-$ destroys gelation,[37] we presume that an imposed R−S−S−R dihedral angle of 90° favors hydrogen-bonding contacts (a presumption borne out by X-ray data to follow). Two factors impede gelation: water solubility and crystallinity. Thus, as mentioned, the highly water-soluble diacetyl-L-cystine does not gelate. Water insolubility is promoted by aroyl groups, which might also contribute π/π stacking to the stability of the fibers. That the latter is not essential is shown by the fact that the dioctanoyl-L-cystine is a good gelator. Hydrophobic forces may, in addition to the water-insolubilizing effect of the octanoyl groups, be playing a role here. Crystallinity, the second enemy of gelation, depends on complex solid-state forces that are difficult to define. The best gelators are compounds which, although water-insoluble, are not so insoluble that they precipitate or crystallize rapidly. Under nonequilibrium constraints, the gelators are able to grow into long, linear arrays that remain dispersed within the water.

X-ray Crystallography. The ability to recrystallize **3** from ether, and to thereby obtain X-ray structures, provides a valuable, albeit nondefinitive, insight into how the L-cystine derivatives might self-assemble. X-ray-quality crystals from a water/DMSO system, which would perhaps have given a greater insight into gel fiber structure, could not be obtained. X-ray structures of two polymorphic forms of **3** are given in Figure 2. These two crystal forms were found side-by-side in chromatography columns and could be separated physically. The structure in Figure 2a is similar to that obtained for **2** in an earlier paper.[37] Thus, the molecules stack linearly with the aid of hydrogen bonds between the carboxyl carbonyl and the aromatic amide NH. A donor/acceptor combination on one side of the S−S linkage hydrogen-bonds to a lower molecule, while the pair on the other side hydrogen-bonds to an upper molecule. Carboxylic acid protons are involved in interfiber hydrogen-bonding with aromatic amide carbonyls (see Supporting Information for details). The aromatic rings of two adjacent molecules are parallel to each other but oriented with the nitro groups displaced 60° from one another. It was this general structure that led us to convert the α-carbonyls into α-carboxamides in order to beneficially enhance the accepting ability of the carbonyl.

One motivating reason for testing the nitro compound was that nitros should enhance the hydrogen-bonding acidity of the critical NH protons. This turned out to be the case. The average N(H)···O distance in the solid state, according to the X-rays, is 3.085 Å for toluoyl derivative **2** but only 2.936 Å for nitrobenzoyl derivative **3**. As it turned out, however, the nitros do not improve the gels but, instead, lead to crystallization. A major problem in gel design, therefore, is to make structural alterations that favor gelation without inadvertently shifting the propensity to self-assemble into the crystalline domain.

A polymorph of **3** in Figure 2b has a rather different packing. In this case, both aromatic amides of a molecule provide carbonyls to hydrogen-bond with NH protons in the unit directly below it. Concurrently, the same aromatic amides of the molecule donate NH protons to amide carbonyls in the unit directly above it. Unlike the situation in Figure 2a, the α-carboxyl carbonyls are engaged only in weak hydrogen bonds to α-CH protons. A single ether molecule per molecule of **3** (not shown) joins two fibers lying side-by-side. Polymorphism in the crystalline state emphasizes the ever-present possibility that the gels themselves are composed of polymorphic structures.[46]

It is possible, of course, that a third packing mode characterizes the gel fibers of the compounds in Table 2. But assuming for simplicity that this is not the case, then both morphologies in Figure 2 demand the presence of the aromatic amide NH proton. One would predict, therefore, that substitution of this proton by a methyl would be fatal to gel formations. It turns out that such a compound (**13**) does indeed fail to form gels. Unfortunately, the results are ambiguous because, according to the NMR, **13** exists in two s-cis/s-trans isomers of roughly equal concentration (see below). Judging from the fact that DL-cystine derivatives do not gelate (unpublished observations),[40] one cannot exclude the possibility that the presence of a mixture suffices in and of itself to prevent gelation.

Microscopy. We now turn to the microscopic properties of the gels. Gel fibers (dried by graded dehydration into ethanol followed by critical point drying from liquid CO_2) were coated

(46) Furman, I.; Weiss, R. G. *Langmuir* **1993**, *9*, 2084.

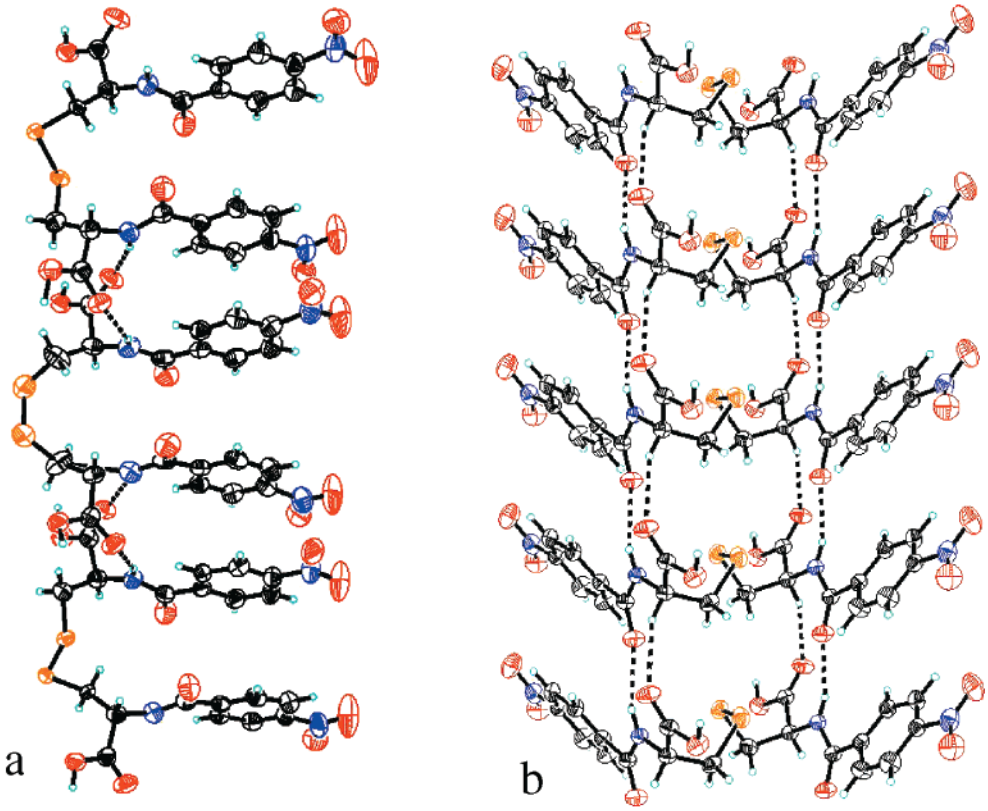

Figure 2. ORTEP diagrams (30% probability) of recrystallized **3** (from diethyl ether), demonstrating the polymorphic nature of the structure. (a) Neat crystals, similar to those of **2**,[37] arranged with a cross-hydrogen-bonding pattern between the acid carbonyl and the amide proton. N(H)···O distances (and N—H—O angles) alternate between 2.987 (161.1°) and 2.885 Å (149.2°). Aromatic rings are parallel, with nitro groups on adjacent molecules displaced 60° from one another. Acid proton−amide carbonyl hyrdogen-bonding occurs between fibers (see Supporting Information). (b) Alternative crystalline molecular organization, incorporating one equivalent of ether (H-bonded to acid protons, not shown). Note intermolecular hydrogen-bonding between aromatic amide carbonyls and aromatic amide NH. N(H)···O distance is 3.093 Å (N—H—O angle = 154.7°); C(H)···O distance is 3.259 Å (C—H—O angle = 158.2°).

with Au/Pd and observed by conventional scanning electron microscopy (SEM). Some of the gels contracted slightly (∼10%) during dehydration. All of the gel-forming derivatives showed fibrous aggregates of varying morphology ranging from ∼50 to 300 nm in width (Figure 3). Filaments from a dried 1 mM sample of **5** are shown in Figure 3a,b. The fibers tend to be roughly linear over moderate distances and randomly oriented. Fibers of **7**, on the other hand, are less defined and more interconnected (Figure 3c). Gels of **7** also contain fibrous clusters, 300 nm wide and 2−4 μm long, which may account for the relative opacity of this gel (Figure 3d). Since clusters are not as effective in entraining solvent as are individual fibers, one also would expect **7** to have a higher minimum gelation concentration, as is the case (Table 2).

Cryo-high-resolution SEM permits a glimpse at this aqueous colloidal system without the prior removal of the liquid phase.[47] Thus, gels of **5** (3 mM, 10% DMSO) were frozen in liquid ethane, fractured, sputter-coated with 1 nm of chromium, and observed in the upper stage of a dual-stage field-emission SEM. The resulting fibers are quite similar in appearance and size to those recorded from the dried gels. Occasional regions of long-range order, where fibers are roughly parallel, are evident (Figure 4).

What does one see by electron microscopy with derivative **8**—a compound that does not gelate water, but instead forms insoluble clumps (Figure 5a)? At higher magnification, these clumps show fine fibers emanating from central nucleation sites (Figure 5b). Thus, **8** retains the propensity to self-assemble into fibers; its failure to gelate stems mainly from a collective insolubility of non-independent fibers. Fine-tuning of gel preparations (including varying H_2O/DMSO ratios) could not coerce **8** to form a gel.

Simple light microscopy of **5** (75/25 H_2O/DMSO) in Figure 6 reveals another important characteristic of the gels: two different fiber morphologies are evident. One type of fiber is thin and linear, whereas the other type of fiber is thick and curved. Both seem to radiate from central points.[8,9] In view of the two crystal forms (Figure 2), polymorphic aggregation is perhaps not surprising.

Rheology.[48] Let us summarize up to this point. Fourteen potential L-cystine-based gelators were synthesized. The compounds were assessed according to their gelation ability, minimum gelation concentration, and gelation time. Structure/activity relationships among the diverse compounds, coupled with suggestive X-ray data, led to reasonable speculations about the molecular associations accompanying the self-assembly into fibers. That fibers do, in fact, form was shown clearly by electron microscopy.

Now, the present paper is entitled "Anatomy of a Gel". If we are to live up to the broad sweep of this title, then the behavior of the fibers must be more fully described. What happens to fibers when they are exposed to mechanical stress?

(47) Apkarian, R. P.; Caran, K. L.; Robinson, K. A. *Microsc. Microanal.* **1999**, *5*, 197.

(48) Barnes, H. A.; Hutton, J. F.; Walters, K. *An Introduction to Rheology*; Elsevier Science B.V.: Amsterdam, 1989; pp 37−54.

(49) Shusterman, A. J.; McDougal, P. G.; Glasfield, A. *J. Chem. Educ.* **1997**, *74*, 1222.

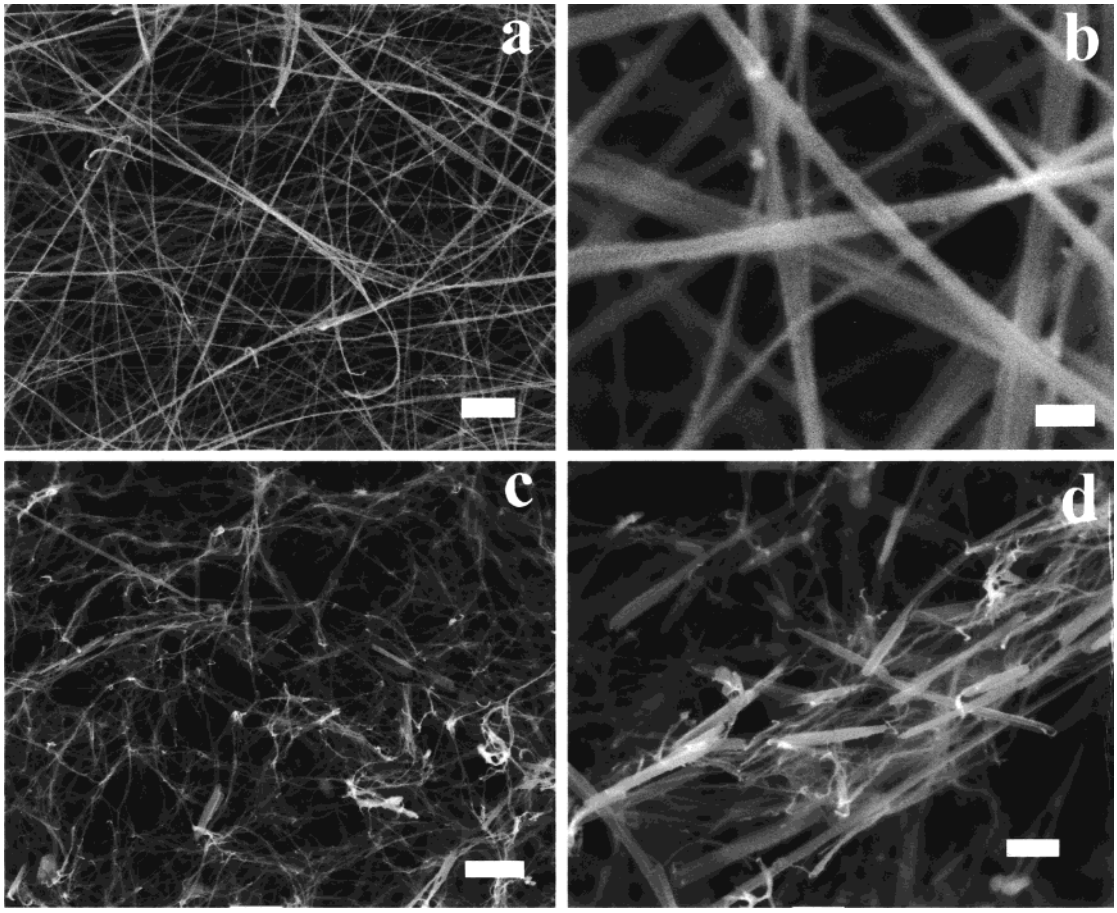

Figure 3. SEM images of fibers obtained from the dehydration and critical point drying of gels of H_2O/DMSO (95/5) gels. (a) Relatively straight fibers from a 1 mM gel of **5** (bar = 2 μm). (b) Higher magnification of fibers from the same gel (bar = 300 nm). (c) Less ordered fibers from a 2 mM gel of **7** (bar = 2 μm). (d) A cluster of fibers from the sample in (c). These aggregates may account for the opacity of gels of **7** (bar = 1 μm).

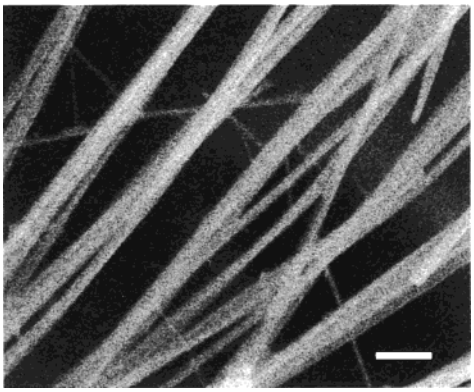

Figure 4. Cryo-HRSEM image of a frozen hydrated 3 mM gel of **5** (10% DMSO). Fibers range in size from ~50 to 300 nm (bar = 1 μm).

How does gelator concentration affect gel rigidity? How do the various gels compare with regard to their "yield stress"? What are the effects of temperature and cosolvent upon fiber dynamics? Such questions fall into the province of rheology, a subject which we now confront. Although textbooks have warned that "rheology is not an easy branch of science", we felt that useful rheological information was within reach.

Our work used a Bohlin controlled-stress rheometer employing a cone-and-plate configuration. A thin layer of gel is placed between a round flat plate at the bottom and a round conical plate (40 mm diameter), fixed to a rotatable shaft, at the top. The cone rotates back and forth at 0.1−10 Hz and at a constant specified torque. The torque is converted directly into "stress" (expressed in pascal units). A position sensor on the oscillating shaft measures the amplitude of the gel's deformation to give the unitless "strain". Gel deformation under the applied stress is assumed to be free from turbulence.

When a sinusoidal shear stress is applied to an ideal Hookean solid, the resulting strain will be in phase (i.e., the phase angle = 0°). For ideal Newtonian liquids, stress and strain will be 90° out of phase. All real materials are "viscoelastic", with phase angles between 0° and 90°.

The complex modulus G^* is defined as the ratio of the amplitudes of stress/strain in an oscillatory experiment. G^* is comprised of two useful components: (a) G', the "storage" (or "elastic") modulus which represents the ability of the deformed material to "snap back" to its original geometry, and (b) G'', the "loss" (or "viscous") modulus which represents the tendency of a material to flow under stress. The rheometer automatically gives G' and G'' in units of pascals as calculated from the measured phase angle (δ) according to the equations below. Clearly, $G' = G^*$ for an ideal solid ($\delta = 0°$), and $G'' = G^*$ for an ideal liquid ($\delta = 90°$). Since $\delta < 10°$ for most of our gels, they have large G' values and can be considered, therefore, rather "solid-like".

$$G' = G^* \cos \delta$$

$$G'' = G^* \sin \delta$$

Gels were subjected to a nondestructive frequency sweep in which an initial stress of 3 Pa was allowed to adjust to a constant

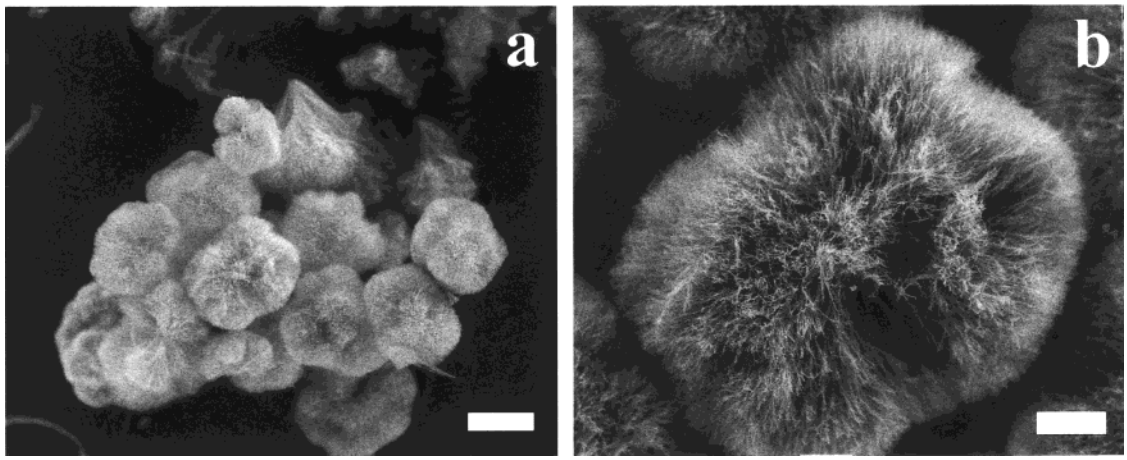

Figure 5. SEM images of a dendritic, fibrous precipitate obtained from an attempted gelation of **8**. (a) A cluster (bar = 100 μm). (b) Higher magnification of one member of the cluster reveals its fibrous nature (bar = 25 μm).

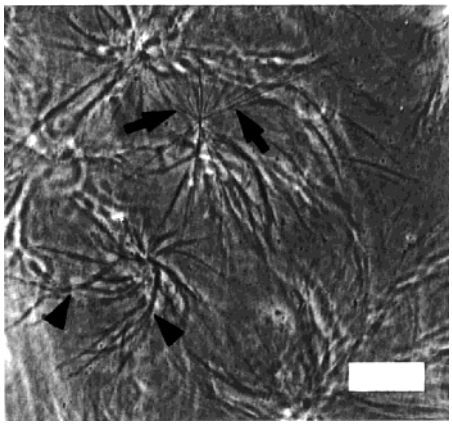

Figure 6. Light micrograph of a 1.0 mM gel of **5** (75/25 H_2O/DMSO). Note two different fiber morphologies: (1) thick and curved (arrowheads) and (2) thin and linear (arrows), suggesting polymorphic aggregation.

strain of 0.001. As can be seen in Figure 7a, a gel of 1 mM **6** (10% DMSO) has G' and G'' parameters that are virtually independent of the oscillation frequency. This is true of the other gels as well. Note that G' is an order of magnitude greater than G'' (as is the case for all the gels), demonstrating the dominant elastic behavior of the systems. Figure 7b plots G' and G'' vs the imposed stress (σ) for the same gel using a 1-Hz oscillation. At a so-called "yield stress" (designated σ_y) of 135 Pa, the gel breaks under the applied force and begins to flow. Each gel has its own particular σ_y according to its strength, as will be discussed later.

Plots of G' vs [gelator] for gels in 75/25 H_2O/DMSO (Figure 8a) and in 90/10 H_2O/DMSO (Figure 8b) contain a wealth of information. (Such plots were obtained for all our gelators, but for the sake of digestibility we are focusing on only a few representative compounds.) (a) Comparison of **5** in the two solvent systems shows that the elastic modulus at a constant concentration increases with diminishing cosolvent. This is intuitively reasonable. Thus, since the gelator is soluble and nongelating in DMSO, the presence of DMSO must adversely affect the integrity of the fibers. Whether the fibers are fewer in number, shorter, or thinner is not known. (b) Rather minor structural variations can have a large impact on gel rigidity. For example, amide **5** is a far better gelator than the corresponding acid **1** (as we had surmised qualitatively in Table 2 and now show quantitatively in Figure 8b). Indeed, compound **1**, the classical gelator, fails to form a viable gel at concentrations up to 20 mM in 75/25 H_2O/DMSO. Figure 8b supports a gelation model, such as Figure 2a, in which a carbonyl oxygen plays a prominent role in fiber formation. (c) The case of compound **10** is instructive. As can be seen in Figure 8a, its G' values, which vary from 51 to 1600 Pa, fall on the baseline when a scale adequate for the other gelators is used. Yet, according to Table 2, **10** is the best gelator with regard to minimum gel concentration (0.25 mM) and gelation time (<30 s). What is the origin of this apparent disparity? Why is it that although 0.25 mM suffices for **10** to form a physically stable gel (i.e., one that will not flow out of an inverted beaker), the gel has, in fact, limited elastic strength when investigated rheologically?

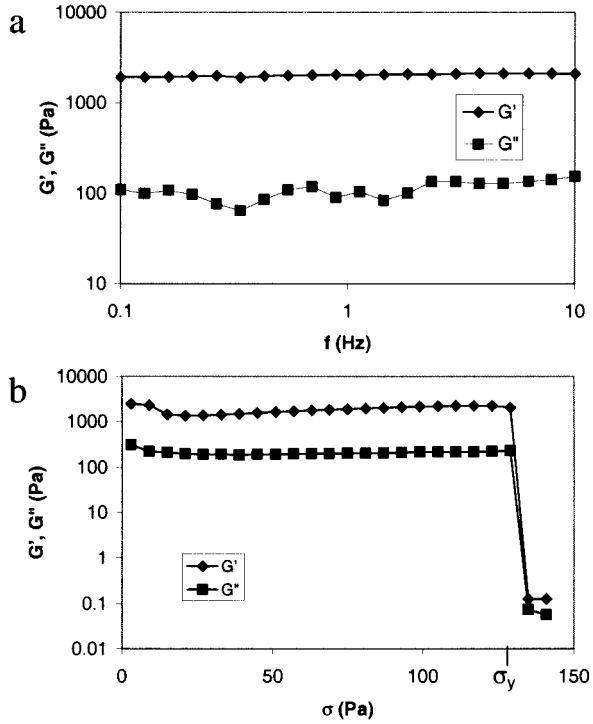

Figure 7. Viscoelastic properties of a 1 mM gel of **6** (10% DMSO). (a) Frequency sweep using a constant target strain of 0.001. Note that G' (♦) is an order of magnitude greater than G'' (■), both values remaining essentially constant from 0.1 to 10 Hz. (b) The amplitude sweep (f = 1 Hz) shows only a small dependence of G' and G'' on the stress amplitude until the yield stress (σ_y, 135 Pa) is reached. Above the yield stress, gels break and begin to flow.

The answers may lie in the kinetics. Thus, gels were prepared

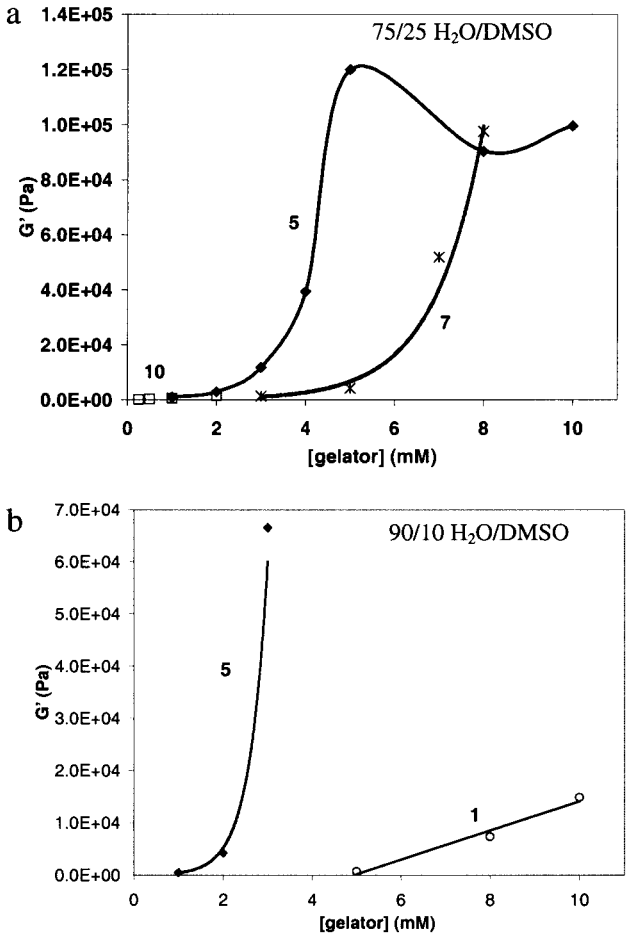

Figure 8. Elastic modulus (G') vs gelator concentration for selected gels from (a) 75/25 H_2O/DMSO and (b) 90/10 H_2O/DMSO. G' generally increases with increasing gelator concentration up to a certain point (see text). Note that gels of **10** (25% DMSO) are stable even at 0.25 mM concentration.

by adding a DMSO solution of gelator to hot water and allowing the system to cool. With compound **10**, gelation is almost immediate, even at higher temperatures. The speed of fiber growth may determine the fiber length just as the speed of crystallization determines crystal size. Compound **10** forms gelating fibers almost instantly, but the gelating fibers are probably short, and, as a consequence, the gel is not rheologically robust. In other words, the propensity to gelate does not necessarily reflect the quality of the ensuing gel. The fact is driven home clearly by the behavior of **5** at higher concentrations, where G' actually decreases (Figure 8a). High concentrations, above a certain limit, tend to accelerate gelation but diminish the elastic modulus. Gels from the various L-cystine derivatives can be legitimately compared only in the sense that they were all prepared under conditions as similar as possible.

The yield stress (σ_y), where the stress finally becomes sufficient to break the gel, was mentioned earlier (Figure 7b). In general, the yield stress increases with concentration (although the function can be complicated owing, we presume, to factors mentioned in the previous paragraph). In any event, at 3 mM gelator (75/25 H_2O/DMSO), σ_y has the following values, in decreasing order for several derivatives: **5** (>600 Pa, the rheometer maximum); **6** (380 Pa); **14**, **11**, and **7** (<40 Pa). Perhaps the comparison between amides **5**, **6**, and **7**, which differ only in the para-substituent on the aromatic ring, is the most illuminating. Gel **7** succumbs to the applied stress at a σ_y an order of magnitude smaller than that for gel **5**; gel **6** is

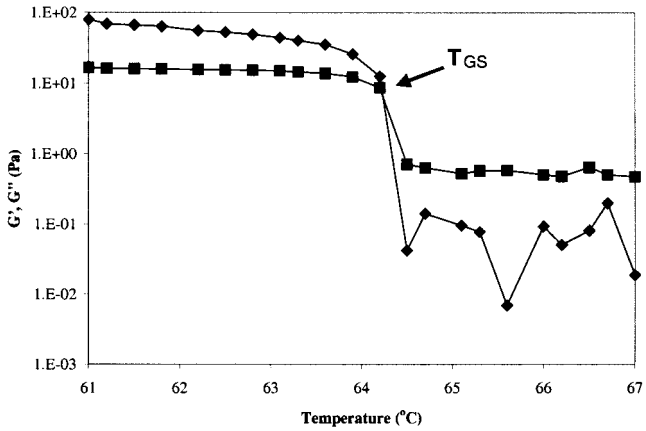

Figure 9. Example of transition temperature (T_{GS}) as determined by temperature-sweep oscillation rheology (1 mM gel of **5**, 25% DMSO). T_{GS} is given by the temperature at which the elastic modulus, G' (◆), drops below the viscous modulus, G''(■), i.e. the gel breaks, under the applied stress of 3 Pa.

intermediate between the two. It seems unlikely that the *p*-OCH_3 and *p*-CH_3 groups destabilize the gel by adversely affecting the π/π overlap within the fibers. More plausibly, the substituents sterically impede the side-by-side alignment of the fibers or, alternatively, lower the monomer solubility and therefore accelerate fiber formation and reduce the average fiber length. Whatever the correct explanation, the remarkable sensitivity of gelation to small structural changes is a noteworthy feature of our physical gels and, perhaps, physical gels in general.

No "anatomy of a gel" is even semicomplete without a discussion of thermal stability, and we will complete our survey with this topic. The gel-to-sol transition temperatures (T_{GS}) were measured rheologically by subjecting an equilibrated gel to a small, discontinuous (2 s on, 10 s off) oscillating stress (1 Hz, 3 Pa) and slowly increasing the temperature from 25 to 90 °C. The point at which the loss modulus, G'', exceeded the storage modulus, G' (i.e., where the gel had broken), was recorded as T_{GS}. Since T_{GS} depends on the experimental design (the greater the stress, the lower the T_{GS}), T_{GS} values reported here are useful for comparison purposes only. In any event, a transition is observed at T_{GS} as both G' and G'' decrease sharply and the gel becomes more "liquid-like" than "solid-like" (Figure 9). It is at this temperature that the system is no longer sufficiently robust to resist the applied stress.

Values of T_{GS} for several gelators are plotted as a function of gelator concentration in Figure 10. Gels **5**, **6**, **10**, and **11**, at only 3 mM concentration, are stable at 90 °C (our highest temperature). Gels of **10** are stable at 90 °C at an astounding 0.25 mM. For comparison purposes, we have included the classical dibenzoyl-L-cystine **1** (dotted line), which required 10% DMSO (rather than the 25% DMSO used for all the others) to form a gel. Even with this special treatment, gel **1** could not reach a $T_{GS} = 80$ °C at 10 mM. Once again, the dramatic effect of the α-carboxylic acid-to-α-carboxamide conversion is evident.

One might think that the sharp breaks in G' and G'' vs temperature plots (Figure 9) provide evidence for sudden phase changes. Differential scanning calorimetry (DSC) tells us otherwise. Thus, DSC scans in both directions gave no clear endothermic or exothermic peaks. These data point strongly to a continuous gel-to-sol conversion upon heating and a sol-to-gel conversion upon cooling. The reason that Figure 9 plots have such sharp breaks is that, upon heating a gel, the gel suddenly loses its ability to withstand an applied torque,

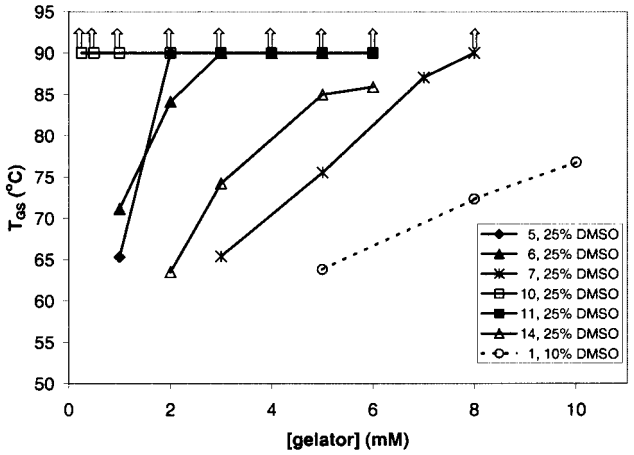

Figure 10. Average T_{GS} values of several gels, determined rheologically as described in Figure 9, plotted against gelator concentration. Arrows indicate that the T_{GS} values lie above 90 °C. Note that gels of **10** are stable at 90 °C, even at an amazingly low 0.25 mM. In contrast, gel **1** fails to reach a T_{GS} = 80 °C even at 10 mM and 10% DMSO.

whereupon a "catastrophe" occurs. Nature is full of such events. When pressure is applied on a paper stapler, nothing happens until the pressure suddenly exceeds the ability of a staple to maintain its geometry.

Thus concludes our anatomy. We have used the multiple tools of organic synthesis, X-rays, electron microscopy, light microscopy, rheology, and calorimetry, and, nonetheless, the precise anatomical features of gels are still elusive. Yet we know a great deal more about our gels, and gels in general, than when we began, and this alone justifies the effort. If our gelators, which function at amazingly low concentrations and high temperatures, prove to have commercial applications (as may well be the case), all the better.

Experimental Section

General Considerations. Melting points were conducted on a Thomas-Hoover capillary melting point apparatus and are uncorrected. Solvents were reagent grade. Reagents were purchased from Aldrich, Sigma, or Fluka (as noted) and used without further purification except for benzoyl chloride, which was distilled prior to use. No attempt was made to optimize yields. Mass spectra measurements were performed by the Mass Spectroscopy Center (Emory University), electron microscopy imaging at the Integrated Microscopy and Microanalytical Facility (Emory University), and NMR spectra measurements (recorded on a Mercury 300, Inova 400 or Omega 600 instrument as indicated) at the NMR Center (Emoy University). Residual solvent peaks were used as NMR reference. X-ray data were collected at room temperature using Cu Kα graphite-monochromated radiation (1.54178 Å) on a Bruker P4/RA single-crystal X-ray diffractometer (Emory University). Atlantic Microlab, Inc. (Norcross, GA) performed elemental analyses. All final products were dried in a vacuum oven (50 °C) over P_2O_5.

General Methods Used for Benzoylation Reactions. (A) L-Cystine, 2 N NaOH, 3% EtOH, and Et_2O were combined in a round-bottom flask and cooled in an ice bath. The aromatic acyl chloride (neat liquid or an Et_2O solution of the solid) and additional 2 N NaOH were added dropwise to the rapidly stirring mixture, after which it was allowed to warm to room temperature. Once the reaction was complete, H_2O was added to dissolve any formed precipitate, and the aqueous layer was washed several times with Et_2O. The product was precipitated by acidification (1 N HCl) of the warm (50 °C) solution. (B) The dihydrohalide salt of L-cystine derivative (methyl ester or primary, secondary, or tertiary amide), anhydrous sodium acetate, water, and Et_2O were combined in a round-bottom flask and cooled in an ice bath. The aromatic acyl chloride (neat liquid or an Et_2O solution of the solid) was added dropwise to the rapidly stirring mixture. Additional water or Et_2O was sometimes needed to break up the formed precipitate. The reaction was allowed to warm to room temperature and run for an allotted amount of time, after which the filtered precipitate (often gelatinous) was washed with water. (C) L-Cystine diamide dihydrochloride (**15**), DMSO, $CHCl_3$, and triethylamine were combined and cooled over an ice bath. The aromatic acyl chloride (neat liquid or a $CHCl_3$ solution of the solid) was added dropwise to the stirring solution. The reaction was allowed to warm to room temperature.

***N,N′*-Dibenzoyl-L-cystine (1).[41] Benzoylation Method A.** L-Cystine (Acros, 2.4 g, 0.01 mol), diethyl ether (10 mL), 3% EtOH (31 mL), 2 N NaOH (10.5 + 12.5 mL), benzoyl chloride (Aldrich, 2.5 mL, 0.022 mol), reaction time ∼20 h. The filtered precipitate was washed with hot water, and dried yielding 1.275 g (28% yield) of white crystalline flaky solid. mp 178−180 °C (ref 180−181 °C). A commercial compound (Fluka) was used in some gel preparations.

***N,N′*-Di(*p*-nitrobenzoyl)-L-cystine (3). Benzoylation Method A.** L-Cystine (4.94 g, 0.025 mol), Et_2O (20 mL + 60 mL), 3% EtOH (60 mL), 2 N NaOH (22 + 28 mL), and *p*-nitrobenzoyl chloride (Aldrich, 10.2 g, 0.055 mol) were reacted for ∼24 h. The filtered solid product was extracted with ethyl acetate and dried with Na_2SO_4. The solvent was removed to yield 9.754 g of crude dry product (slightly yellow). The solid was purified by dry-column flash chromatography[49] using ether as the eluant. Two distinct crystal types of the product had formed (long colorless needles and light yellow compact crystals) which were found to be randomly distributed throughout the fractions after ∼2 d. X-ray structures revealed their distinct crystal morphologies (see Results and Discussion). The colorless needles incorporated one ether of crystallization, while the yellow crystals were neat: 1.686 g (13% yield); mp = 208−209 °C. FAB-HRMS $(M - H)^-$: 537.04061 (calculated: 537.03864). ^{1}H NMR (400 MHz, acetone-d_6): δ CH_2 (2H, 3.295 ppm, dd, ^3J = 9.6 Hz, ^2J = 14.0 Hz), δ CH_2 (2H, 3.493 ppm, dd, ^3J = 4.4 Hz, ^2J = 14.0 Hz), δ CH (2H, 5.048 ppm, m), δ Ar−H (4H, 8.118 ppm, ^3J = 8.7 Hz), δ Ar−H (4H, 8.273 ppm, ^3J = 8.85 Hz), δ NH (2H, 8.467 ppm, ^3J = 8.0 Hz). ^{13}C NMR (acetone-d_6): δ 40.499, 53.317, 124.397, 129.699, 131.787, 150.568, 166.313, 171.861 ppm. IR (KBr): 3700−2800 (br), 1738, 1731, 1704, 1693, 1644, 1599, 1535, 1520, 1486, 1422, 1348, 1306, 1291, 1246, 1216, 1107, 1013, 867, 845, 799, 713 cm^{-1}. Anal. Calcd for $C_{20}H_{18}N_4O_{10}S_2$: C, 44.61; H, 3.37; N, 10.40; S, 11.91. Found: C, 43.74; H, 3.46; N, 9.62; S, 11.74.

L-Cystine diamide dihydrochloride (15) was prepared according to the method of Martin et al.[42] with minor modifications. NH_3 (∼150 mL) was condensed in a 1-L round-bottom flask at −78 °C. L-Cystine dimethyl ester dihydrochloride (Sigma, 10 g, 0.0293 mol) was added with stirring. The reaction was allowed to slowly warm to −33 °C. The NH_3 was refluxed on a coldfinger cooled to −78 °C, protected with a KOH drying tube. After ∼4 h, the NH_3 was allowed to evaporate, yielding a crude yellow solid which was heated to 50 °C in vacuo. Methanol was added, and the solution was warmed to 60 °C, which dissolved all but a trace of the crude solid, which was removed by filtration through cotton. The product was precipitated by acidification with excess HCl in MeOH. The solid was filtered and washed with cold MeOH to yield 7.48 g (82% yield) of slightly off-white powder: mp = 222−224 °C (lit. mp = 226.5−227.5 °C). The solid was recrystallized from 66% aqueous MeOH. ^{1}H NMR (400 MHz, D_2O, presaturated): δ CH_2 (2H, 3.326 ppm, dd, ^3J = 8.4 Hz, ^2J = 15.2 Hz), δ CH_2 (2H, 3.446 ppm, dd, ^3J = 4.8 Hz, ^2J = 15.2 Hz), δ CH (2H, 4.414 ppm, dd, ^3J = 8.4, 4.8 Hz), δ NH_2 (7.486, 8.067 ppm).

***N,N′*-Di(*p*-nitrobenzoyl)-L-cystine Diamide (4). Benzoylation Method B.** L-Cystine diamide dihydrochloride (**15**, 1.00 g, 3.21 mmol), NaOAc (1.053 g, 12.84 mmol), H_2O (30 mL), Et_2O (5 + 10 mL), and *p*-nitrobenzoyl chloride (Acros, 1.49 g, 8.03 mmol) were reacted for ∼12 h. The solid was washed with MeOH, purified by trituration in hot MeOH, and dried, yielding 0.778 g of a light green solid (45% yield): mp = 218−219 °C. FAB-HRMS $(M + H)^+$: 537.0857 (calculated: 537.0862). ^{1}H NMR (400 MHz, DMSO-d_6): δ CH_2 (2H, 3.002 ppm, dd, ^3J = 10.23 Hz, ^2J = 13.42 Hz), δ CH_2 (2H, 3.289 ppm, dd, ^3J = 4.42 Hz, ^2J = 13.58 Hz), δ CH (2H, 4.702 ppm, m), δ NH_2 (4H, 7.286, 7.621 ppm), δ Ar−H (4H, 8.062 ppm, d, ^3J = 8.86 Hz), δ Ar−H (4H, 8.274 ppm, d, ^3J = 8.85 Hz), δ NH (2H, 9.987 ppm, d, ^3J = 8.09 Hz). ^{13}C NMR (DMSO-d_6): δ 171.740, 164.867, 149.043, 139.583, 129.054, 123.410, 52.596 ppm (methylene signal

obscured by solvent peaks). Anal. Calcd for $C_{20}H_{22}N_6O_8S_2$: C, 44.77; H, 3.76; N, 15.66; S, 11.95. Found: C, 44.58; H, 3.79; N, 15.50; S, 12.08.

***N,N′*-Dibenzoyl-L-cystine Diamide (5). Benzoylation Method B.** L-Cystine diamide dihydrochloride (**15**, 1.00 g, 3.21 mmol), NaOAc (1.053 g, 12.84 mmol), H_2O (20 mL), Et_2O (10 mL), and benzoyl chloride (0.84 mL, 7.23 mmol) were reacted overnight. The product was purified by trituration in hot MeOH, yielding 750 mg of a white solid (1.68 mmol, 52% yield): mp = 239−240 °C. FAB-HRMS (M + Li)$^+$: 453.12392 (calculated: 453.12427). ^{1}H NMR (300 MHz, DMSO-d_6): δ CH_2 (2H, 3.055 ppm, dd, ^3J = 10.35 Hz, ^2J = 13.35 Hz), δ CH_2 (2H, 3.264 ppm, dd, ^3J = 13.35 Hz, ^2J = 4.35 Hz), δ CH (2H, 4.713 ppm, m), δ NH_2 (2H, 7.244, s), δ NH_2, Ar−H, Ar−H (8H, 7.423−7.530 ppm, m), δ Ar−H (4H, 7.868, ^3J = 7.2 Hz, d), δ NH (2H, 8.589, ^3J = 8.4 Hz, d). ^{13}C NMR (DMSO-d_6): δ 172.038, 166.470, 133.986, 131.344, 128.163, 127.499, 52.460, 33.224 ppm. Anal. Calcd for $C_{20}H_{22}N_4O_4S_2$: C, 53.80; H, 4.97; N, 12.55; S, 14.36. Found: C, 53.76; H, 5.01; N, 12.45; S, 14.43.

***N,N′*-Di(*p*-toluoyl)-L-cystine Diamide (6). Benzoylation Method C.** L-Cystine diamide dihydrochloride (**15**, 0.500 g, 1.61 mmol), DMSO (10 mL), chloroform (10 mL), NEt_3 (1.2 mL, 8.66 mmol), and *p*-toluoyl chloride (Aldrich, 0.468 mL, 2.59 mmol) were reacted for 8 h. The volume of the milky white reaction mixture was increased with $CHCl_3$ (∼80 mL). The suspension was filtered, washed with $CHCl_3$, and allowed to dry overnight. The solid was purified by trituration in hot MeOH. After drying, it yielded 0.643 g (1.35 mmol, 84% yield): mp = 227−231 °C. FAB-HRMS (M + Li)$^+$: 481.15722 (calculated: 481.15555). ^{1}H NMR (400 MHz, DMSO-d_6): δ CH_3 (6H, 2.341 ppm), δ CH_2 (2H, 3.049 ppm, dd, ^3J = 10.4 Hz, ^2J = 13.3 Hz), δ CH_2 (2H, 3.244 ppm, dd, ^3J = 4.3 Hz, ^2J = 13.4 Hz), δ CH (2H, 4.698 ppm, m), δ Ar−H, NH_2 (6H, 7.245 ppm, m), δ NH_2 (2H, 7.521 ppm, s), δ Ar−H (4H, 7.769 ppm, d, ^3J = 7.9 Hz), δ NH (2H, 8.502 ppm, d, ^3J = 8.1 Hz). ^{13}C NMR (DMSO-d_6): δ 21.016, 39.99 (somewhat obscured by solvent peaks), 52.436, 127.560, 128.713, 131.201, 141.252, 166.354, 172.157 ppm. Anal. Calcd for $C_{22}H_{26}N_4O_4S_2$: C, 55.68; H, 5.52; N, 11.81; S, 13.51. Found: C, 55.50; H, 5.54; N, 11.65; S, 13.59.

***N,N′*-Di(*p*-anisoyl)-L-cystine Diamide (7). Benzoylation Method C.** L-Cystine diamide dihydrochloride (**15**, 0.500 g, 1.61 mmol), DMSO (8 mL), $CHCl_3$ (8 + 5 mL), NEt_3 (1.2 mL, 8.66 mmol), and *p*-anisoyl chloride (Aldrich, 0.603 g, 3.53 mmol) were reacted for 5.5 h. The reaction volume was increased with $CHCl_3$ (25 mL), filtered, and washed with a large volume of $CHCl_3$. The product was triturated in methanol and dried, yielding a white solid (760 mg, 1.50 mmol, 93% yield): mp = 216−218 °C. FAB-HRMS (M + Li)$^+$: 513.1459 (calculated: 513.1454). ^{1}H NMR (400 MHz, DMSO-d_6): δ CH_2 (2H, 3.044 ppm, dd, ^3J = 10.5 Hz, ^2J = 13.3 Hz), δ CH_2 (2H, 3.235 ppm, dd, ^3J = 4.2 Hz, ^2J = 13.3 Hz), δ CH_3 (6H, 3.796 ppm, s), δ CH (2H, 4.684 ppm, m), δ Ar−H (4H, 6.972 ppm, d, ^3J = 8.7 Hz), δ NH_2 (2H, 7.223 ppm, s), δ NH_2 (2H, 7.503 ppm, s), δ Ar−H (4H, 7.843 ppm, d, ^3J = 8.7 Hz), δ NH (2H, 8.431 ppm, d, ^3J = 8.1 Hz). ^{13}C NMR (DMSO-d_6): δ 52.452, 55.346, 113.367, 126.178, 129.373, 161.678, 165.933, 172.203 ppm. Anal. Calcd for $C_{22}H_{26}N_4O_6S_2 \cdot H_2O$: C, 50.37; H, 5.38; N, 10.68; S, 12.22. Found: C, 50.42; H, 5.00; N, 10.62; S, 12.36.

***N,N′*-Di(3,5-dimethoxybenzoyl)-L-cystine Diamide (8). Benzoylation Method C.** L-Cystine diamide dihydrochloride (**15**, 0.500 g, 1.61 mmol), DMSO (10 mL), $CHCl_3$ (10 + 4 mL), NEt_3 (1.2 mL, 8.66 mmol), and 3,5-dimethoxybenzoyl chloride (Aldrich, 0.711 g, 3.54 mmol) were reacted overnight. The $CHCl_3$ and excess NEt_3 were removed by rotary evaporation, followed by a Kugelrohr distillation, which removed the DMSO, revealing a light brown solid. The crude material was washed with chloroform, triturated in hot MeOH, and dried to yield 0.703 g (1.24 mmol, 77% yield) of pure white solid: mp = 224−225 °C. FAB-HRMS (M + Li)$^+$: 573.1682 (calculated: 573.1665). ^{1}H NMR (400 MHz, DMSO-d_6): δ CH_2 (2H, 3.032 ppm, dd, ^3J = 10.3 Hz, ^2J = 13.2 Hz), δ CH_2 (2H, 3.242 ppm, dd, ^3J = 4.3 Hz, ^2J = 13.5 Hz), δ CH_3 (12H, 3,774 ppm, s), δ CH (2H, 4.693 ppm, m), δ Ar−H (2H, 6.639 ppm, s), δ Ar−H (4H, 7.030 ppm, d, ^4J = 2.1 Hz), δ NH_2 (2H, 7.242 ppm, s), δ NH_2 (2H, 7.521 ppm, s), δ NH (2H, 8.568 ppm, d, ^3J = 8.1 Hz). ^{13}C NMR (DMSO-d_6): δ 39.81 (somewhat obscured by solvent peaks), 52.459, 55.433, 103.307, 105.454, 136.041, 160.217, 166.035, 172.013 ppm. Anal. Calcd for $C_{24}H_{30}N_4O_8S_2$: C, 50.87; H, 5.34; N, 9.89; S, 11.32. Found: C, 50.77; H, 5.33; N, 9.80; S, 11.43.

***N,N′*-Di(3,5-dinitrobenzoyl)-L-cystine Diamide (9). Benzoylation Method C.** L-Cystine diamide dihydrochloride (**15**, 0.500 g, 1.61 mmol), DMSO (10 mL), $CHCl_3$ (10 + 5 mL), NEt_3 (1.2 mL, 8.66 mmol), and 3,5-dinitrobenzoyl chloride (Aldrich, 0.814 mg, 3.53 mmol) were reacted for ∼4 h. The solution turned pink upon addition of the acyl chloride. After 3 h at room temperature (the solution appears tannish-pink), the $CHCl_3$ and excess NEt_3 were removed by rotary evaporation, after which $HNEt_3^+ Cl^-$ was filtered out. DMSO was removed by Kugelrohr distillation, to reveal a dark brown solid material. The solid was washed with $CHCl_3$, yielding a tan solid, which was purified by trituration in MeOH. The crystalline off-white solid was dried overnight (0.198 g, 0.31 mmol, 19% yield): mp = 217−219 °C. FAB-HRMS (M + Li)$^+$: 633.0654 (calculated: 633.0646). ^{1}H NMR (400 MHz, DMSO-d_6): δ CH_2 (2H, 3.011 ppm, dd, ^3J = 13.3 Hz, ^2J = 4.4 Hz), δ CH_2 (2H, 3.3 ppm, dd, ^2J = 4.4 Hz), δ CH (2H, 4.741 ppm, m), δ NH_2 (2H, 7.312 ppm, s), δ NH_2 (2H, 7.713 ppm, s), δ Ar−H (2H, 8.930 ppm, t, ^4J = 2.1 Hz), δ Ar−H (4H, 9.035 ppm, d, ^4J = 2.1 Hz), δ NH (2H, 9.435 ppm, d, ^3J = 8.2 Hz). ^{13}C NMR (DMSO-d_6): δ 52.687, 120.922, 127.780, 136.519, 148.019, 162.364, 171.383 ppm (methylene signal obscured by solvent peaks). Anal. Calcd for $C_{20}H_{18}N_8O_{12}S_2$: C, 50.37; H, 5.38; N, 10.68; S, 12.22. Found: C, 50.42; H, 5.00; N, 10.62; S, 12.36.

***N,N′*-Di(2-naphthoyl)-L-cystine Diamide (10). Benzoylation Method C.** L-Cystine diamide dihydrochloride (**15**, 0.500 g, 1.61 mmol), DMSO (10 mL), $CHCl_3$ (10 + 5 mL), NEt_3 (1.2 mmol, 8.66 mmol), and 2-naphthoyl chloride (Aldrich, 0.673 g, 3.54 mmol) were reacted for ∼1.5 h. The precipitate was filtered, washed with $CHCl_3$, and dried overnight, yielding a slightly yellow solid. Trituration in hot MeOH followed by drying yielded 0.6871 g (1.26 mmol, 78% yield) of white solid: mp = 236−237 °C. FAB-HRMS (M + Li)$^+$: 553.15686 (calculated: 553.15558). ^{1}H NMR (400 MHz, DMSO-d_6): δ CH_2 (2H, 3.121 ppm, dd, ^3J = 10.23 Hz, ^2J = 13.43 Hz), δ CH_2 (2H, 3.329 ppm, dd, ^3J = 4.6 Hz, ^2J = 13.5 Hz), δ CH (2H, 4.798 ppm, m), δ NH_2 (2H, 7.300 ppm, s), δ Ar−H, NH_2 (6H, 7.583−7.619 ppm, m), δ Ar−H (8H, 7.919−8.002 ppm, m), δ Ar−H (2H, 8.483 ppm, s), δ NH (2H, 8.795 ppm, d, ^3J = 8.2 Hz). ^{13}C NMR (DMSO-d_6): δ 52.588, 124.419, 126.801, 127.560, 127.666, 127.757, 128.811, 128.895, 131.353, 132.050, 134.197, 166.536, 172.112 ppm (methylene signal obscured by solvent peaks). Anal. Calcd for $C_{28}H_{26}N_4O_4S_2$: C, 61.52; H, 4.79; N, 10.25; S, 11.73. Found: C, 61.41; H, 4.85; N, 10.15; S, 11.78.

L-Cystine Dimethylamide Dihydrochloride (16). This compound was prepared using the same method as for **15**, substituting NH_2Me for NH_3. L-Cystine dimethyl ester dihydrochloride (Sigma, 1.0 g, 2.93 mmol) was dissolved in ∼20 mL of anhydrous methylamine at −78 °C (protected with a $CaCl_2$ drying tube). The methylamine solution was allowed to warm to its boiling poing (condensed on −78 °C coldfinger) and react for 3 h, after which the bulk of the excess solvent was allowed to evaporate. Further evaporation at 50 °C under vacuum (aspirator) yielded a thick, clear, colorless oil which was dissolved in methanol and acidified with HCl. Precipitation or crystallization of the di-HCl salt proved unsuccessful, so the excess solvent was removed, and the crude yellow oil was carried on to the next step. (Impurity by ^{1}H NMR: $NH_2Me \cdot HCl$.)

***N,N′*-Dibenzoyl-L-cystine Di(methylamide) (11). Benzoylation Method B.** Crude L-cystine dimethylamide dihydrochloride (**16**, 2.93 mmol, assuming 100% yield), NaOAc (1.06 g, 12.9 mmol), Et_2O (15 mL), and benzoyl chloride (1.50 mL, 12.9 mmol) were reacted for 2.5 h. The crude dry white solid, after being washed with Et_2O, was purified by trituration in hot MeOH. After drying, a pure white solid was obtained (1.01 g, 72% yield after two steps): mp = 275−276 °C dec. FAB-HRMS (M + Li)$^+$: 481.1579 (calculated: 481.1556). ^{1}H NMR (400 MHz, DMSO-d_6): δ CH_3 (6H, 2.601 ppm, d, ^3J = 4.6 Hz), δ CH_2 (2H, 3.034 ppm, dd, ^3J = 10.1 Hz, ^2J = 13.4 Hz), δ CH_2 (2H, 3.231 ppm, dd, ^3J = 4.6 Hz, ^2J = 13.4 Hz), δ CH (2H, 4.707 ppm, m), δ Ar−H (4H, 7.448 ppm, t, ^3J = 7.8 Hz), δ Ar−H (2H, 7.530 ppm, tt, ^3J = 7.3 Hz, ^4J = 1.6 Hz), δ Ar−H (4H, 7.870 ppm, dd, ^3J = 7.8 Hz, ^4J = 1.5 Hz), δ NH (2H, 8.031 ppm, q, ^3J = 4.6 Hz), δ NH_2 (2H,

8.643 ppm, d, ^3J = 7.9 Hz). ^{13}CNMR (DMSO-d_6): δ 25.867, 39.9 (somewhat obscured by solvent peaks), 52.567, 127.591, 128.175, 131.407, 133.910, 166.472, 170.394 ppm. Anal. Calcd for $C_{22}H_{26}N_4O_4S_2$: C, 55.68; H, 5.52; N, 11.81; S, 13.51; O, 13.48. Found: C, 55.68; H, 5.48; N, 11.69; S, 13.62; O, 13.56.

***N,N′*-Di-Z-L-cystine di(dimethylamide) (17)** (Z = Cbz) was made according to the method of Gustus for the preparation of the analogous primary amide.[43] Di-Z-L-cystine (Fluka, 2.0 g, 3.93 mmol) was ground to a fine powder, suspended in anhydrous Et_2O in a 50-mL Erlenmeyer, flask and cooled to 0 °C. PCl_5 (1.8 g, 8.65 mmol, ground to a fine powder) was added, and the suspension was alternately shaken vigorously and cooled (~2-min cycles) for 30 min. The resulting diacyl chloride (white solid) was filtered, washed with cold anhydrous Et_2O, and then suspended in 50 mL of anhydrous Et_2O at −78 °C under N_2. Cold dimethylamine (~2 mL) in Et_2O (10 mL) was added to the suspension under N_2, and the mixture was stirred at −78 °C for 1 h, after which the reaction was allowed to warm to room temperature in a dimethylamine atmosphere. Et_2O and excess $NHMe_2$ were removed under vacuum to reveal a fluffy white solid. Repeated attempts at recrystallization resulted only in an oil, which was carried on to the next step.

L-Cystine Di(dimethylamide) Dihydrobromide (18). The crude *N,N′*-di-Z-L-cystine di(dimethylamide) (**17**) oil was deprotected in 20% HBr in AcOH (10 mL). The clear yellow solution was stirred at room temperature for 1 h, after which the bulk of the AcOH was removed under vacuum, revealing an orange-brown oil. Repeated trituration in room temperature acetone resulted in a crude white solid that was filtered from the colored solution and dried (0.82 g). ^{1}H NMR (D_2O, 400 MHz): δ CH_3 (6H, 2.975 ppm, s), δ CH_3 (6H, 3.151 ppm, s), δ CH_2 (2H, 3.172 ppm, m), δ CH_2 (2H, 3.358 ppm, dd, ^3J = 4 Hz, ^2J = 15 Hz), δ CH (2H, 4.840 ppm, m). ^{13}CNMR (D_2O with acetone for reference): δ 35.656, 36.319, 36.684, 49.438, 166.896 ppm.

***N,N′*-Dibenzoyl-L-cystine Di(dimethylamide) (12). Benzoylation Method B.** Crude L-cystine di(dimethylamide) dihydrobromide (**18**, 0.82 g), NaOAc (0.65 g, 7.92 mmol), H_2O (20 mL), Et_2O (30 mL), and benzoyl chloride (0.63 mL, 5.4 mmol) were reacted for 6 h. Since the ^{1}H NMR showed a mixture of mono- and dibenzoylated products, the crude solid (0.33 g) was dissolved in 10 mL of $CHCl_3$, to which were added benzoyl chloride (58 μL, 0.5 mmol) and triethylamine (55 μL, 0.4 mmol). After reaction overnight, the solvent was removed, and the crude tan solid was suspended in Et_2O and filtered (0.335 g). The product was recrystallized from MeOH/H_2O, yielding 0.188 g of pure needle-shaped crystals after drying (10% overall yield after four steps): mp = 199−200 °C. FAB-HRMS $(M + Li)^+$: 509.1872 (calculated: 509.1869). ^{1}H NMR (300 MHz, $CDCl_3$): δ CH_3 (6H, 2.957 ppm, s), δ CH_3, CH_2 (10H, 3.120−3.275 ppm, m), δ CH (2H, 5.502−5.434 ppm, m), δ Ar−H, δ NH (8H, 7.288−7.497 ppm, m), δ Ar−H (4H, 7.783 ppm, d, ^3J = 7.3 Hz). ^{13}CNMR ($CDCl_3$): δ 36.247, 37.715, 41.843, 48.983, 127.300, 128.613, 131.894, 133.646, 166.784, 170.074 ppm. Anal. Calcd for $C_{24}H_{30}N_4O_4S_2$: C, 57.35; H, 6.02; N, 11.15; O, 12.73; S, 12.76. Found: C, 57.24; H, 6.09; N, 11.02; O, 12.86; S, 12.79.

***N,N′*-Dimethyl-L-cystine (19)** was made according to the method of Keller-Schierlein et al.[44] (*R*)-(−)-Thiazolidine-4-carboxylic acid[50] (Aldrich, 6.66 g, 50 mmol) was dissolved in ammonia at −78 °C, and to this was added 0.9 mL of H_2O. Solid Na was added until the solution remained blue (~3.7 g). The reaction was quenched with NH_4Cl and allowed to warm to room temperature and evaporate overnight. After drying under vacuum, the crude white solid was dissolved in 50 mL of water and acidified to pH 1 with 6 N HCl. The solvent and excess acid were removed under vacuum to reveal a sticky off-white solid. The solid was extracted with absolute EtOH (5 × 50 mL), which yielded a sticky yellow material (7.261 g) after removal of the solvent. The methylated amino acid salt was air-oxidized to the disulfide by dissolving it in 250 mL of water, bringing it to pH 9 with ammonium hydroxide, adding one crystal of iron sulfate ($Fe^{II}SO_4 \cdot 6H_2O$), and bubbling air through the solution overnight. After 13 h, the solution tested negative for thiolates using the nitroprusside reaction.[51] The solution was acidified to pH 6 with 25% AcOH. Addition of 200 mL of absolute EtOH precipitated a thick white solid which was removed by centrifugation (4 °C, 20 000 rpm, 30 min) and washed twice with 50% EtOH. The solid was dissolved in water and lyophilized yielding 1.924 g of fluffy off-white solid. FAB-LRMS $(M + H)^+$: 269.12 (calculated: 269.06). ^{1}H NMR (D_2O, 400 MHz): δ CH_3 (6H, 2.738 ppm, s), δ CH_2 (4H, 3.325 ppm, d, ^3J = 4 Hz), δ CH (2H, 3.937 ppm, ^3J = 4 Hz).

***N,N′*-Dimethyl-*N,N′*-dibenzoyl-L-cystine (13).** This compound was made according to the method of Bloch and Clark[45] with modifications. *N,N′*-Dimethyl-L-cystine (**19**, 1.00 g, 3.73 mmol) and potassium bicarbonate (5.33 g, 53.2 mmol) were dissolved in 10 mL of water to which 10 mL of Et_2O was added. The solution was cooled to 0 °C, and benzoyl chloride (Aldrich, 3.0 mL, 25.8 mmol) was added dropwise with rapid stirring. After the solution was allowed to react overnight and was passed through filter paper, it was acidified with 1 N HCl to pH 3, causing a thick yellow mass to precipitate. The water was decanted off, and the solid was dissolved in acetone. The solvent was removed to yield a slightly sticky yellow solid. Trituration in Et_2O yielded followed by trituration in water and drying yielded 0.671 g of a pure off-white solid containing a ~1:1 mixture of cis and trans amide isomers: mp = 99−119 °C. FAB-HRMS $(M + H)^+$: 477.1161 (calculated: 477.1154). ^{1}H NMR (400 MHz, DMSO-d_6): δ Ar−H (10H, 7.387 ppm, m), δ CH (1H, 5.097, m), δ CH (1H, 4.493 ppm, m), δ CH_2 (4H, 3.242 ppm, m), δ CH_3 (3H, 2.859 ppm, d), δ CH_3 (3H, 2.785 ppm, d). The CH_3 peaks coalesced to a singlet (δ 2.87 ppm) by 75 °C and the CH peaks to a single wide peak (δ 4.92 ppm) by 100 °C in a VT ^{1}H NMR experiment (600 MHz) as exchange between the rotamers became more rapid. Anal. Calcd for $C_{22}H_{24}N_2O_6S_2$: C, 55.45; H, 5.08; N, 5.88; O, 20.14; S, 13.46. Found: C, 55.15; H, 5.04; N, 5.93; O, 20.34; S, 13.40.

***N,N′*-Dibenzoyl-L-cystine Dimethyl Ester (14). Benzoylation Method B.** L-Cystine dimethyl ester dihydrochloride (Sigma, 10.5 g, 30.8 mmol), NaOAc (10.1 g, 123.2 mmol), H_2O (100 mL), Et_2O (100 mL), and benzoyl chloride (7.87 mL, 67.8 mmol) were reacted for 4 h. Trituration in Et_2O and drying yielded 8.181 g (56% yield) of pure dry white solid: mp = 169−172 °C. FAB-HRMS $(M + H)^+$: 477.1151 (calculated: 477.1154). ^{1}H NMR (300 MHz, DMSO-d_6): δ CH_2 (2H, 3.150 ppm, dd, ^3J = 9.9 Hz, ^2J = 13.8 Hz), δ CH_2 (2H, 3.295 ppm, dd, ^3J = 4.5 Hz, ^2J = 13.8 Hz), δ CH_3 (6H, 3.664 ppm, s), δ CH (2H, 4.776 ppm, m), δ Ar−H (6H, 7.491 ppm, m), δ Ar−H (4H, 7.848 ppm, d, ^3J = 7.3 Hz), δ NH (2H, 8.955 ppm, d, ^3J = 7.6 Hz). ^{13}C NMR (DMSO-d_6): δ 38.580 (somewhat obscured by solvent peaks), 51.814, 52.258, 127.250, 128.179, 131.477, 133.275, 166.284, 170.860 ppm. Anal. Calcd for $C_{22}H_{24}N_2O_6S_2$: C, 55.45; H, 5.08; N, 5.88; O, 20.14; S, 13.46. Found: C, 55.44; H, 5.03; N, 5.88; O, 20.23; S, 13.32.

Physical Studies on Gels. (a) Gelation Tests. Each of the compounds tested was dissolved in an appropriate amount of warm DMSO in a glass vial. The solution was heated to >90 °C in a water bath. Hot (>90 °C) Milli-Q-purified water (18 MΩ·cm) was added to the vial, bringing the final volume to 5 mL. The vial was sealed (screw cap), removed from the water bath, and allowed to cool slowly (undisturbed) to room temperature.

(b) Rheology. Rheological measurements were carried out on a Bohlin CSR-10 constant stress rheometer, using a cone-and-plate geometry (truncated 4/40 cone, 4° cone angle, 40-mm diameter). A Neslab circulating water bath or a Peltier device controlled the temperature of the bottom plate. The gap distance was fixed at 150 μm. Gels (1.25-mL total volume) were prepared by mixing a DMSO solution of the gelator with hot Milli-Q water on the heated (90 °C) plate, lowering the cone, and cooling the system to 25 °C at ~3 °C/min. A low-viscosity oil (viscosity standard S3, 3.494 mPa·s at 25 °C, Cannon Instrument Co.) was used around the edges of the gel, which acted as a moisture barrier (impeding evaporation). An oscillatory shear stress (2 s on, 10 s off) was applied to the gel typically after it remained at 25 °C for 1 h. A constant frequency of 1 Hz and a uniform stress (3−50 Pa, depending on the strength of the gel) was employed. The level of stress used (≥3 Pa, instrument minimum) was approximately the minimum value able to generate a strain of at least 4×10^{-4} (approximately the minimum measurable strain for 4/40 cone) for each gel. The shear strain (γ), complex modulus (G^*), storage modulus (G'), loss modulus (G''), complex viscosity (η^*), and phase angle (δ) were

(50) Ratner, S.; Clarke, H. T. *J. Am. Chem. Soc.* **1937**, *59*, 200.

(51) Szaciłowski, K.; Stochel, G.; Stasicka, Z. *New J. Chem.* **1997**, *21*, 893.

monitored and recorded as a function of time, and each run was allowed to continue until these values remained approximately constant. All gels were subjected to frequency sweeps (0.1−10 Hz, auto stress mode, target strain = 0.001), while stress amplitude sweeps (3−600 Pa, 1 Hz) were run with selected samples of each concentration. Temperature sweep rheological methods are described below.

(c) Temperature-Sweep Oscillation Rheology. Gels formed on the rheometer and tested as above were used in temperature-sweep experiments. (Those subjected to an amplitude sweep were not used for temperature sweep tests.) Gels were subjected to a small oscillating stress (3 Pa), and the temperature was slowly (3 °C/min) increased from 25 to 90 °C. The temperature at which the gel could no longer support the applied stress (when $G'' > G'$) was recorded as the transition temperature (T_{GS}).

(d) Differential Scanning Calorimetry. Gels (500 μL) were prepared by mixing a DMSO solution of the gelator and Milli-Q water to each of three hermetically sealed DSC cells at room temperature. Gels were homogenized at 100° C for 20 min and then cooled to 10 °C prior to each test. DSC runs were recorded from 10 to 100 °C and from 100 to 10 °C at 10 °C/h. Baselines were run with 500 μL of the corresponding of water/DMSO mixture.

(e) Light Microscopy. Eighty-microliter gels were prepared by adding Milli-Q water to DMSO solutions of **5** on microscope slides with small glass O-rings cemented to them (height = 1.5 mm, inside diameter = 8 mm). Glass coverslips were placed on top, and the gels were allowed to set. Phase-contrast images were recorded on a Nikon Diaphot-TMD inverted microscope (40× objective) equipped with an Optronics DEI-750TD Peltier-cooled 3-CCD color camera.

(f) Electron Microscopy. Gels, jellies, or precipitates (5 mL) were prepared as explained in the Gelation Tests section above. Samples were successively dehydrated in a graded ethanol series (30, 50, 70, 90, 100, 100, 100%) for 15−30 min each. The ethanol was slowly replaced with liquid CO_2 in a critical point drying (CPD) apparatus at 0 °C. Once the exchange was complete (∼3 h), the temperature was increased, bringing CO_2 above its critical point, after which the CO_2 was slowly released as a gas. The dried gels were mounted onto SEM stubs with carbon tape, coated with ∼10 nm Au/Pd (60/40), and observed on the lower stage of a DS-130 LaB_6 scanning electron microscope (SEM) using a 10- or 19-kV accelerating voltage. Images were digitally recorded and processed using Adobe Photoshop.

A detailed procedure for cryo-high-resolution (HR) SEM sample preparation and imaging of frozen, hydrated samples has been published[47] and is summarized as follows. A small portion of a gel (∼10 μL cut from the rest of the gel with a razor) was placed onto a gold planchet (Balzers), frozen in liquid ethane at its melting point (∼ −183 °C), and stored under liquid nitrogen (LN_2). The sample was loaded into a prechilled cryopreparation chamber (cooled to ∼ −170 °C with LN_2), attached to an Oxford CT-3500 cold stage, fractured with a cold blade, and rinsed with LN_2. The sample (with stage shutters closed to avoid frost contamination) was quickly transferred to a Denton DV-602 magnetron sputter coater, where it was coated with 1 nm Cr. Samples were observed in the upper stage of an ISI DS-130F Schottky field-emission SEM (where they were warmed to −110 °C to allow any ice condensed on the surface of the Cr to sublime) using a 25-kV accelerating voltage and processed as above.

Acknowledgment. We thank the staff at Bohlin Instruments and Dr. Thomas Oomann (Kimberly Clark Corp.) for their advice on and assistance with the rheology, Dr. Robert P. Apkarian for imaging the cryo-HRSEM samples, Dr. Nikolai A. Khanjin and Mr. Bao Do for their determination of and assistance with the X-ray crystal structures, Dr. David Goldsmith for photographing the gels, and Dr. Vincent P. Conticello for helpful discussions. In addition, we thank the National Institutes of Health (Grant GM21457) for funding.

Supporting Information Available: Additional ORTEP diagram of recrystallized **3** (morph from Figure 2a) showing inter-fiber hydrogen-bonding (PDF), and X-ray crystallographic files (CIF) for both polymorphs of **3**. This material is available free of charge via the Internet at http://pubs.acs.org.

JA0016811